Upregulation of a nuclear factor-kappa B-interacting immune gene network in mice cochleae with age-related hearing loss

Authors: Kensuke Uraguchi, Yukihide Maeda, Junko Takahara, Ryotaro Omichi, Shohei Fujimoto, Shin Kariya, Kazunori Nishizaki and Mizuo Ando

Affiliation (All authors):

Department of Otolaryngology- Head and Neck Surgery, Okayama University Graduate School of Medicine, Dentistry and Pharmaceutical Sciences, 2-5-1 Shikata, Kita-Ku, Okayama 700-8558, Japan

Corresponding author:

Yukihide Maeda, MD, Ph.D.

Department of Otolaryngology- Head and Neck Surgery, Okayama University Graduate School of Medicine, Dentistry and Pharmaceutical Sciences, 2-5-1 Shikata, Kita-Ku, Okayama 700-8558, Japan

Tel: 001-81-86-235-7307; Fax: 001-81-86-235-7308; email: yamayuki@cc.okayama-u.ac.jp

Abstract

Epidemiological data suggest that inflammation and innate immunity play significant roles in the pathogenesis of age-related hearing loss (ARHL) in humans. In this mouse study, real-time RT-PCR array targeting 84 immune-related genes revealed that the expressions of 40 genes (47.6%) were differentially regulated with greater than a twofold change in 12-month-old cochleae with ARHL relative to young control mice, 33 (39.3%) of which were upregulated. These differentially regulated genes (DEGs) were involved in functional pathways for cytokine–cytokine receptor interaction, chemokine signaling, TNF signaling, and Toll-like receptor signaling. An NF-κB subunit, *Nfkb1*, was upregulated in aged cochleae, and bioinformatic analyses predicted that NF-κB would interact with the genomic regulatory regions of eight upregulated DEGs, including *Tnf* and *Ptgs2*. In aging cochleae, major proinflammatory molecules, *IL1B* and *IL18rap*, were upregulated by 6 months of age and thereafter. Remarkable upregulations of seven immune-related genes (*Casp1*, *IL18r1*, *IL1B*, *Card9*, *Clec4e*, *Ifit1*, and *Tlr9*) occurred at an advanced stage (between 9 and 12 months of age) of ARHL. Immunohistochemistry analysis of cochlear sections from the 12-month-old mice indicated that IL-18r1 and IL-1B were localized to the spiral ligament, spiral limbus, and organ of Corti. The two NF-κB-interacting inflammatory molecules, TNFα and PTGS2, immunolocalized ubiquitously in cochlear structures, including the lateral wall (the stria vascularis and spiral ligament), in the histological sections of aged cochleae. IBA1-positive

macrophages were observed in the stria vascularis and spiral ligament in aged mice. Therefore, inflammatory and immune reactions are modulated in aged cochlear tissues with ARHL.

Key words: Age-related hearing loss, mouse cochlea, RT-PCR array, real-time RT-PCR, immunohistochemistry, inflammaging, innate immunity, nuclear factor-kappa B

Introduction

Age-related hearing loss (ARHL; namely presbycusis) is a major medical and social issue in developed countries with rapidly aging populations. In the United States, approximately one third of the total population aged 65–74 years experiences ARHL, and nearly half of the population aged >75 years has hearing difficulties [1]. In Japan, which is the most rapidly aging country in the world, persons aged ≥65 years represented 28.1% of the total population in 2018, and this percentage is anticipated to reach approximately 40% by 2065 [2]. ARHL significantly affects the health of older adults, leading to difficulty in communication, mental disabilities such as depression and dementia, low quality of life, and decreased social activity [3]. The progression of ARHL is thought to involve multiple molecular mechanisms in the cochlea; therefore, it is important to elucidate the pathologic mechanisms underlying ARHL in the cochlea so that preventive and therapeutic treatments for ARHL can be developed.

Schuknecht divided the classical human histopathological findings of ARHL in the cochleae

into four categories—sensory presbycusis, neural presbycusis, metabolic presbycusis, and conductive cochlear loss—according to the site of abnormalities in the microscopic cellular structures of the cochleae, including the hair cells, stria vascularis, and spiral neurons [4]. Experimental studies in the cochleae of mice with ARHL found that the cumulative effect of oxidative stress damages mitochondrial DNA, and in turn, mutations/deletions in mitochondrial DNA lead to a decline in mitochondrial function and apoptosis in cochlear cells [5, 6].

Epidemiological data suggest that inflammation and innate immunity play significant roles in the pathogenesis of ARHL in humans. Epidemiological studies have reported that elevations in serum C-reactive protein levels, neutrophil counts, and inflammatory cytokine interleukin (IL)-6 levels are associated with a higher risk of ARHL and worse hearing levels in older adults [7, 8]. However, data from animal experiments mechanistically demonstrating the involvement of inflammation and innate immunity in the pathology of ARHL in the cochleae are scarce [9, 10].

As an animal model of ARHL, inbred C57BL/6J mice exhibit the ARHL phenotype as early as 6 months of age [11]. Technically, gene expression studies by means of DNA microarray and next-generation sequencing (RNA-seq) allow genome-wide analyses of approximately 22,000 mice genes; however, real-time RT-PCR outperforms these technologies by enabling more accurate quantification of specific gene expressions encoding proteins with known functions. Therefore, in the first step of this study, the expression levels of 84 inflammatory

and immune-related genes were analyzed by a real-time RT-PCR array in the cochleae of 12-month-old and 6–7-week-old C57BL/6J mice, and as many as 33 immune-related genes were found to be upregulated in cochleae of the older mice. In the second step, at which time points of the aging process (3-, 6-, 9-, and 12-month-old C57BL/6J mice) such upregulations of immune-related genes were observed was investigated. In the third step, immunohistochemical experiments were performed to clarify the histological localization of such immune-related gene/protein expressions in mice cochleae. These data help provide a more precise understanding of how the immune process occurs in the cochleae of aging mice with ARHL.

Materials and Methods

Dissection of mice cochlear tissues and RNA extraction

All animal experiments were performed in compliance with the ethical standards approved by Okayama University's Committee on the Use and Care of Animals (protocol Nos.: OKU-2018847, 2019396, 2019397, 2019398, and 2020549; principal investigator: Y.M.) and adhered to national and international standards of animal care.

For the extraction of cochlear RNA samples to perform PCR-based gene expression experiments, 6–7-week-old [young control mice], 12–13-week-old [3 months], 25–26-week-old [6 months], 38–39-week-old [9 months], and 52–54-week-old [12 months]) male C57BL/6J

mice were obtained from Charles River Laboratories (Yokohama, Japan). For the dissection of cochlear samples from mice at 6–7 weeks (*n*=6) and 3 (*n*=6), 6 (*n*=6), 9 (*n*=6), and 12 months (*n*=6), deeply anesthetized mice (intraperitoneal ketamine [80 mg/kg] and xylazine [8 mg/kg]) were euthanized via cervical dislocation. The cochlear tissues were promptly dissected into collection tubes containing RNA later reagent (Qiagen, Hilden, Germany). The samples were then incubated in RNA later (Qiagen) at 4 °C for 24 h and stored frozen until RNA purification. The tissues were homogenized, and total RNA was purified using a miRNeasy mini column (Qiagen). The quantity and quality of the RNA samples were assessed using a spectrophotometer (NanoDrop™ One; Thermo Fisher Scientific, Waltham, MA, USA) and the Agilent 2100 Bioanalyzer system (Agilent Technologies, Santa Clara, CA, USA). One cochlear tissue was collected from a mouse, and >0.6 μg of total RNA with an RNA integrity number >8.0 was purified per one cochlear tissue.

Hearing levels in mice with ARHL

It was verified that 6- and 12-month-old male C57BL/6J mice exhibited significant ARHL based on click-auditory brainstem response (c-ABR) thresholds compared with younger 6–7-week-old male C57BL/6J mice. Hearing levels were assessed using the c-ABR as previously described [12]. Under anesthesia with intraperitoneal ketamine (80 mg/kg) and xylazine (8 mg/kg), click sounds were delivered to the ear in 5-dB steps from 90 dB sound pressure level (SPL) to 0 dB. c-ABR was recorded by needle electrodes inserted into the vertex and

postauricular area as an averaged record of 1000 responses for each SPL. The c-ABR threshold was defined as the minimum SPL at which the c-ABR was clearly recognized. c-ABR thresholds in the young control mice (*n*=7), 6-month-old mice (*n*=10), and 12-month-old mice (*n*=8) were compared using the Kruskal–Wallis and Mann–Whitney *U* tests.

Real-time RT-PCR array (RT^2 Profiler™)

Between the cochleae of 12-month-old and 6–7-week-old mice, the differences in expression levels of 84 key genes actively involved in inflammatory and immune functions were analyzed using the RT^2 Profiler™ PCR array (Qiagen). The RT^2 Profiler™ PCR array is a 96-well plate spotted with specific primers for 84 targeted genes to each well. The targeted genes were those encoding cytokines (including chemokines and interleukins), their receptors and signaling molecules, and genes involved in acute, chronic, and intracellular inflammatory responses. The entire list of the 84 genes analyzed in the array is provided as supporting information.

A cDNA library was synthesized by reverse-transcription of the RNA samples (500 ng) from the 12-month-old and 6–7-week-old cochleae using the RT^2 First Strand Kit (Qiagen). With the cDNA libraries used as templates for the PCR reactions, the expression levels of 84 key genes related to inflammatory and immune functions were profiled by the mouse inflammation and autoimmunity RT^2 Profiler™ PCR array (PAMM-077Z; Qiagen) using the LightCycler 480 real-time PCR system (Roche Diagnostics K.K., Tokyo, Japan) according to the

manufacturer's instructions. The PCR array experiment was performed in triplicate, and the gene expression levels were estimated using RT^2 Profiler™ PCR array data analysis software (Qiagen). Differences in expression levels between the 12-month-old and 6–7-week-old mice were calculated based on the difference in ⊿Ct values normalized to the levels of a housekeeping gene of heat shock protein 90-beta. *P*-values for differences in the expression levels between the 12-month-old and 6–7-week-old mice were assessed by Student's *t*-test. If the expression level showed greater than a twofold change or less than a 0.5-fold change, and was significantly different ($P<0.05$), the gene was considered upregulated (greater than a twofold change) or downregulated (less than a 0.5-fold change) in the 12-month-old compared with the 6–7-week-old mice.

Gene specific real-time RT-PCR

The expression levels of nine inflammatory and immune-related genes were compared between the cochleae of 6–7-week-old (young control mice) and 3-, 6-, 9-, and 12-month-old mice by means of gene-specific real-time RT-PCR to investigate the time point when these inflammatory and immune-related gene expressions were modulated. The following nine immune-related genes were selected for the real-time RT-PCR analyses because our preliminary data, by means of next-generation sequencing (RNA-seq), suggested that these genes with important immune functions were upregulated in the cochleae of 12-month-old mice. In our preliminary data by RNA-seq, 800 genes were either upregulated (452 genes) or

153 downregulated (348 genes) more than twofold in the aged cochleae of 12-month-old mice,
154 compared with the cochleae of 6–7-week-old mice, and their functions were analyzed by
155 bioinformatic analyses.

156 A cDNA library was synthesized by the reverse-transcription of the cochlear RNA samples
157 (typically 500 ng) using the RT^2 First Strand Kit (Qiagen). Real-time PCR was performed using
158 RT^2 SYBR Green qPCR Mastermix (Qiagen) and the specific primers for inflammatory and
159 immune-related genes *Casp1* (PPM02921E; RT^2 qPCR Primer Assay, Qiagen), *IL18r1*
160 (PPM03555B), *IL18rap* (PPM03137A), *IL1B* (PPM03109F), *Card9* (PPM40791A), *Clec4e*
161 (PPM06261F), *Ifit1* (1PPM05530E), *Ifit3* (PPM06008B), and *Tlr9* (PPM04221A) using a
162 thermal cycler (PTC-200; CFX Connect™, BioRad, Hercules, CA, USA). The gene expression
163 level in each sample was calculated according to the ΔΔCt method with normalization to the
164 level of the internal control, *Actb* (beta actin; PPM02945B).

165 The levels in 6–7-week-old and 3-, 6-, 9-, and 12-month-old cochleae were expressed as
166 the mean ± standard deviation (SD) and compared using analysis of variance and the
167 Bonferroni post-hoc test (n=6 for each time point, P<0.05). The specific primers for each gene
168 were designed and experimentally verified for real-time PCR analyses by Qiagen. Information
169 on the gene-specific primers is available on the Qiagen homepage
170 (https://geneglobe.qiagen.com/product-groups/rt2-qpcr-primer-assays).

171 **Bioinformatic analyses of functions of the differentially**

expressed genes (DEGs)

Real-time RT-PCR array experiments generated a list of differentially expressed genes (DEGs), which were significantly upregulated (greater than a twofold change) or downregulated (less than a 0.5-fold change) in the cochleae of the 12-month-old mice as compared with the 6–7-week-old mice ($P<0.05$ by *t*-test).

First, the biological pathways associated with these DEGs were investigated using the Kyoto Encyclopedia of Genes and Genomics (KEGG) pathway analysis with the David Bioinformatics Resources 6.8 web-based genome database (https://david.ncifcrf.gov/) [13, 14]. The KEGG pathway is the annotation of functional gene pathways involving a group of genes. If a subset of DEGs is identified in abundance in a KEGG pathway with a *P*-value <0.05 and a false discovery rate (FDR) <0.05, these DEGs are considered as significantly enriching this pathway with a specific biological function.

Second, which transcription factors might regulate the expression of these DEGs was investigated to help understand how these DEGs are regulated by the upstream gene transcription mechanisms. Candidates for the transcription factors regulating these DEGs were identified based on predictions by the web-based Molecular Signatures Database 7.2 (MSigDB; https://www.gsea-msigdb.org/) [15, 16]. This analysis assessed the presence of DNA sequences targeted by transcription factors in the genomic regulatory region of the DEGs based on a *P*-value <0.05 and an FDR <0.05.

Third, the gene expression network of DEGs was studied using the web-based STRING 11.0 analysis tool (https://string-db.org) [17]. STRING is a program that analyzes the mutual relationships of proteins evidenced by their experimentally verified interactions, co-expressions, and co-citations in curated databases and PubMed abstracts, and visualizes the genes/protein association networks. The list of the DEGs was subjected to STRING with a medium confidence score of 0.4.

Immunohistochemistry

Immunohistochemical analysis of paraffin sections of cochleae from 12-month-old mice (*n*=3) and 6–7-week-old mice (*n*=3) was performed as previously described, with minor modifications [12]. After heat-mediated antigen retrieval, reactions were performed using anti–IL-18r1 antibody (ab231554; Abcam, Cambridge, UK, diluted 1/50), anti–IL-1B antibody (ab9722; Abcam, diluted 1/100), anti-TNFα antibody (ab 6671; Abcam, diluted 1/50), and anti-PTGS2 antibody (ab 15191; Abcam, diluted 1/100) at 4 °C overnight, followed by visualization using the ABC method (Vectastain Elite ABC Kit; Vector Laboratories, Burlingame, CA, USA). Rabbit polyclonal antibody raised against IBA1 (Ionized calcium binding adaptor protein 1), a macrophage/microglia-specific calcium-binding protein [18], was used to detect macrophages by immunohistochemistry (A3160; ABclonal, Tokyo, Japan, diluted 1/50). Immunofluorescent visualization of specific IL-18r1, IL-1B, TNFα and PTGS2 immunoreactivities was also performed using Alexa Fluor 568 donkey anti-rabbit IgG (A10042; Thermo Fisher Scientific,

diluted 1/200) at 4 °C for 30 m. Tissue autofluorescence was eliminated using an autofluorescence quenching kit (TrueVIEW kit, Vector Laboratories) following the manufacturer's protocol, and nuclear counterstaining was performed using diamidino-2-phenylindole (DAPI). The specificity of the primary antibodies to IL-18r1, IL-1B, TNFα, and PTGS2 was verified by western blotting by the manufacturer (Abcam). As a negative control, sections were incubated with nonspecific rabbit IgG (5 μg/mL) and then visualized. Light and fluorescent microscopic images were acquired using a fluorescent microscope (BX-51-54; Olympus, Tokyo, Japan).

Results

Hearing levels in mice with ARHL

As shown in Fig 1, the c-ABR threshold was significantly higher in 6-month-old mice (63.0±14.9 dB SPL, mean±SD, *n*=10) and 12-month-old mice (66.9±13.6 dB SPL, *n*=8) than in 6–7-week-old mice (40±2.9, *n*=7) ($P<0.01$), confirming that 6- and 12-month-old mice exhibited significant ARHL. The c-ABR thresholds in the 6- and 12-month-old mice were shifted by 23.0 and 26.9 dB, respectively, compared with the younger control mice.

Fig 1. Click-auditory brainstem response (c-ABR) thresholds demonstrating age-related hearing loss in male C57BL/6J mice. The mean ± standard deviation c-ABR

threshold was significantly higher in 6-month-old mice (63.0±14.9 dB sound pressure level, *n*=10) and 12-month-old mice (66.9±13.6, *n*=8) than in 6–7-week-old mice (40±2.9, *n*=7) (*P*<0.01, Kruskal–Wallis and Mann–Whitney *U* tests).

Real-time RT-PCR array and bioinformatic analyses of DEGs

A volcano plot (Fig 2) shows the gene expression profiles of 84 genes in the inflammatory and immune pathways analyzed by the real-time RT-PCR array. Each gene was plotted as a function of the ratio of expression levels between the 12-month-old and 6–7-week-old mice (the x-axis) and *P*-values for the differential expression levels between the two age groups (the y-axis). Among the 84 targeted genes, as many as 40 were significantly upregulated (33 genes) or downregulated (7 genes) with greater than a twofold change in the cochleae of 12-month-old compared with 6–7-week-old mice (*P*<0.05). Table 1 summarizes the gene symbols and names of these 40 DEGs from among the 84 analyzed immune-related genes.

Fig 2. A volcano plot showing the ratios of the gene expression levels in the cochleae of 12-month-old mice relative to young control mice. Data of 84 key genes involved in inflammatory and immune functions are plotted. Forty of the 84 genes are differentially expressed with greater than twofold upregulation (greater than a twofold change, 33 genes) or downregulation (less than a 0.5-fold change, 7 genes), as well as significant *P*-values to

indicate differential expression levels (P<0.05, t-test) between the cochleae of 12-month-old vs. 6–7-week-old mice (young control mice). The x-axis indicates Log2 (fold change of 12-month-old mice/young control mice) showing the relative expression levels. The y-axis represents –Log10 (P-value) to assess significant differences between the two groups (n=3 for each gene in the 12-month-old and young control mice).

Table 1. Inflammatory and immune-related genes upregulated or downregulated in the cochleae of 12-month-old compared with 6–7-week-old mice.

Upregulated genes

Gene symbol	Gene name	P-value (t-test)	Fold change
Ccl12	Chemokine (C-C motif) ligand 12	0.00034	3.48
Ccl2	Chemokine (C-C motif) ligand 2	0.00065	3.31
Ccl5	Chemokine (C-C motif) ligand 5	0.00124	3.2
Ccl7	Chemokine (C-C motif) ligand 7	0.00037	2.38
Ccl8	Chemokine (C-C motif) ligand 8	0.00173	11.24
Ccr1	Chemokine (C-C motif) receptor 1	0.00130	2.72
Ccr2	Chemokine (C-C motif) receptor 2	0.00005	3.2
Ccr3	Chemokine (C-C motif) receptor 3	0.00040	2.83
Ccr7	Chemokine (C-C motif) receptor 7	0.00010	3.31
Cxcl10	Chemokine (C-X-C motif) ligand 10	0.00012	3.85
Cxcl9	Chemokine (C-X-C motif) ligand 9	0.00009	5.9
Cxcr1	Chemokine (C-X-C motif) receptor 1	0.00037	4.83
Cxcr2	Chemokine (C-X-C motif) receptor 2	0.00059	3.15
Cxcr4	Chemokine (C-X-C motif) receptor 4	0.00024	3.47
Fasl	Fas ligand (TNF superfamily, member 6)	0.02733	2.67
Ifng	Interferon gamma	0.01286	2.22
Il1a	Interleukin 1 alpha	0.00470	2.32
Il1b	Interleukin 1 beta	0.00053	3.67

Il6	Interleukin 6	0.00002	4.43
Il7	Interleukin 7	0.00342	2.59
Kng1	Kininogen 1	0.00136	4.26
Lta	Lymphotoxin A	0.00301	2.83
Ltb	Lymphotoxin B	0.00140	2.2
Nfkb1	Nuclear factor of kappa light polypeptide gene enhancer in B-cells 1, p105	0.00005	2.03
Nr3c1	Nuclear receptor subfamily 3, group C, member 1	0.00346	2.08
Ptgs2	Prostaglandin-endoperoxide synthase 2	0.00477	2.59
Sele	Selectin, endothelial cell	0.03442	2.05
Tlr1	Toll-like receptor 1	0.00074	4.34
Tlr6	Toll-like receptor 6	0.00108	5.99
Tlr7	Toll-like receptor 7	0.00000	5.04
Tlr9	Toll-like receptor 9	0.00011	3.82
Tnf	Tumor necrosis factor	0.00149	2.06
Tnfsf14	Tumor necrosis factor (ligand) superfamily, member 14	0.00167	2.48
	Downregulated genes		
Ccl1	Chemokine (C-C motif) ligand 1	0.00014	0.39
Ccl20	Chemokine (C-C motif) ligand 20	0.00014	0.39
Crp	C-reactive protein, pentraxin-related	0.00005	0.43
Cxcl3	Chemokine (C-X-C motif) ligand 3	0.00352	0.26
Il17a	Interleukin 17A	0.00017	0.38
Il22	Interleukin 22	0.00014	0.39
Il9	Interleukin 9	0.00011	0.42

Table 1 legend. The expressions of 84 immune-related genes were analyzed by real-time RT-PCR array. As a result, 33 upregulated and 7 downregulated genes were detected with greater than a twofold or less than a 0.5-fold change, respectively, with a *P*-value <0.05 for significantly different expression levels in the 12-month-old relative to the 6–7-week-old mice (*n*=3, *t*-test).

These DEGs were shown to play roles in the biological functions of the top five significant

KEGG functional pathways abundantly enriched by the DEGs, including cytokine–cytokine receptor interaction (involving 29 DEGs; *P*=6.4E-35; FDR=5.9E-33), the chemokine signaling pathway (18 DEGs; *P*=7.0E-18; FDR=3.2E-16), the TNF signaling pathway (13 DEGs; *P*=7.0E-14; FDR=2.2E-12), and the Toll-like receptor signaling pathway (11 DEGs; *P*=3.4E-11; FDR=6.2E-10) (Table 2).

Table 2. Functional gene pathways associated with the differentially expressed genes (DEGs) in 12-month-old relative to 6–7-week-old cochleae (top 5 significant pathways).

	Gene count	*P*-value(<0.05)	FDR(<0.05)
Cytokine-cytokine receptor interaction	29	6.4E-35	5.9E-33
Chemokine signaling pathway	18	7.0E-18	3.2E-16
TNF signaling pathway	13	7.0E-14	2.2E-12
Rheumatoid arthritis	11	4.0E-12	9.2E-11
Toll-like receptor signaling pathway	11	3.4E-11	6.2E-10

Table 2 legend. The biological functions of 40 DEGs identified by the real-time RT-PCR array were significantly associated with these top five KEGG pathways with a *P*-value <0.01 and a false discovery rate (FDR) <0.01.

The analysis of transcription factor targets in the MSigDB database revealed that a transcription factor, nuclear factor-kappa B (NF-κB), was predicted to interact *in-trans* with the genomic regulatory sequences of eight upregulated DEGs: *Ccl5* (chemokine (C-C motif) ligand 5), *Cxcl10* (chemokine (C-X-C motif) ligand 10), *Cxcl9* (chemokine (C-X-C motif) ligand

9), *Il1a* (IL 1 alpha), *Lta* (lymphotoxin A), *Ltb* (lymphotoxin B), *Ptgs2* (prostaglandin-endoperoxide synthase 2), and *Tnf* (tumor necrosis factor), with a *P*-value <0.01 and an FDR <0.01.

Based on the DNA sequence information deposited in the database, the genomic regulatory regions of these eight DEGs contain at least one NF-κB target sequence in the regions spanning up to 4 kb around the transcription starting site of each DEG. Furthermore, a subunit of the NF-κB transcription factor complex, *Nfkb1* (nuclear factor of kappa light polypeptide gene enhancer in B-cells 1, p105), was significantly upregulated in the cochleae of aged compared with young mice in our dataset for the real-time RT-PCR array.

Fig 3, which was created using the STRING program, shows the protein–protein association network of the immune-related DEGs actively controlled in aged cochleae. The figure illustrates that the transcription factor *Nfkb1* is upregulated in aged cochleae, and in turn, NF-κB binds to the genomic regulatory regions of eight upregulated DEGs—*Ccl5*, *Cxcl10*, *Cxcl9*, *Il1a*, *Lta*, *Ltb*, *Ptgs2*, and *Tnf*—which are mutually associated in the network of the 40 immune-related DEGs.

Fig 3. Expression network of 40 differentially regulated genes (DEGs) with inflammatory and immune functions in 12-month-old cochleae. A web-based STRING database (https://string-db.org) computed a graphical representation of the mutual

297 relationships of the 40 immune-related DEGs detected by the real-time RT-PCR array,
298 based on their experimentally verified interactions, co-expressions, and co-citations in
299 curated databases and PubMed abstracts. The figure shows that a transcription factor,
300 *Nfkb1*, is upregulated in aged cochleae, and that NF-κB interacts with the genomic
301 regulatory regions of the eight upregulated DEGs (*Ccl5*, *Cxcl10*, *Cxcl9*, *Il1a*, *Lta*, *Ltb*, *Ptgs2*,
302 and *Tnf*) mutually associated in the expression network of the 40 immune-related DEGs in
303 aged cochleae.
304

305 Gene-specific real-time RT-PCR

306 Fig 4 summarizes the respective mean±SD expression levels of the nine inflammatory and
307 immunity-related genes at each time point: *Casp1* (6–7-week-old mice: 1.01±0.07 -fold
308 change; 3-month-old mice: 1.00±0.05; 6-month-old mice: 0.97±0.04; 9-month-old mice:
309 1.00±0.06; 12-month-old mice: 2.88±0.16), *IL18r1* (1.00±0.07, 1.20±0.06, 1.00±0.05,
310 1.17±0.06, 1.49±0.08), *IL18rap* (1.01±0.12, 0.99±0.15, 1.41±0.25, 1.41±0.12, 1.62±0.07),
311 *IL1B* (1.00±0.07, 1.74±0.12, 2.02±0.14, 1.58±0.06, 3.51±0.29), *Card9* (1.00±0.07, 1.19±0.04,
312 1.36±0.10, 1.08±0.06, 2.58±0.10), *Clec4e* (1.01±0.10, 1.24±0.12, 1.39±0.15, 1.23±0.15,
313 3.39±0.32), *Ifit1* (1.01±0.11, 1.68±0.16, 1.20±0.10, 1.11±0.07, 5.49±0.52), *Ifit3* (1.00±0.09,
314 1.92±0.18, 2.14±0.17, 1.66±0.15, 1.75±0.14), and *Tlr9* (1.00±0.09, 0.95±0.17, 0.71±0.05,
315 1.40±0.09, 3.26±0.33). As shown in the figure, the major proinflammatory molecule *IL1B* was

316 significantly upregulated by more than a 1.5-fold change at the early time point of 3 months
317 and thereafter, as compared with the level at 6–7 weeks. *IL18rap* was significantly upregulated
318 by more than a 1.4-fold change at the time point of 6 months and thereafter. An interferon-
319 induced gene, *Ifit3*, was also upregulated by more than a 1.5-fold change at the time point of
320 3 months and thereafter. Seven out of nine inflammatory and immunity-related genes (except
321 for *IL18rap* and *Ifit3*) examined by gene-specific real-time RT-PCR showed significant and
322 noticeable upregulation between the late time points of 9 and 12 months (P<0.01, n=6 for each
323 time point).
324
325 **Fig 4. Gene-specific real-time RT-PCR of immune-related genes in the cochleae of 6–**
326 **7-week-old (young control) and 3-month-old (3M), 6-month-old (6M), 9-month-old (9M),**
327 **and 12-month-old (12M) mice.** Gene expression levels are analyzed for the nine
328 inflammatory and immune-related genes—*Casp1*, *IL18r1*, *IL18rap, IL1B*, *Card9*, *Clec4e*,
329 *Ifit1*, *Ifit3*, and *Tlr9*—at each age of the mice cochleae. The expressions of the major
330 proinflammatory molecules *IL1B* and *IL18rap* are upregulated by 3M and 6M, respectively,
331 and thereafter during the aging process as compared with the levels in the young control
332 cochleae. *Ifit3* is also upregulated by 3M and thereafter. The expressions of seven of the
333 nine immune-related genes (except for *IL18rap* and *Ifit3*) show significant upregulation
334 between the ages of 9M and 12M (n=6 for each time point, P<0.01 by analysis of variance

and the Bonferroni post-hoc test).

Immunohistochemistry

The IL-18r1 receptor and IL-1B were found to be upregulated in 12-month-old cochleae in the real-time RT-PCR analyses. Immunohistochemical analysis of cochlear histochemical sections from 12-month-old mice demonstrated that both proteins localized in the spiral ligament, spiral limbus, and organ of Corti (upper insets in Fig 5). Because the organ of Corti in 12-month-old C57BL/6 mice showed signs of age-related degeneration in the basal turn of the cochleae in previous studies [19], the organ of Corti in the apical turn was examined in our immunohistochemical analysis in the aged mice. In the cochleae of 6-week-old mice, IL-18r1 and IL-1B localized in the spiral ligament, the spiral limbus, and the organ of Corti (lower insets in Fig 5). Cochlear localization of IL-18r1 and IL-1B was similar between the aged and younger mice.

Fig 5. Immunohistochemical analysis of IL-18 receptor 1 (IL-18r1) and IL-1 beta (IL-1B) expression in aged cochleae. The figures show immunoreactivity to IL-18r1 and IL-1B in the cochleae of 12-month-old and 6-week-old mice. Negative control sections incubated with nonspecific rabbit IgG showed no signals except for background staining in the spiral neurons in sections visualized using the ABC method. Therefore, the signals in

354 the spiral neurons may be due to the nonspecific protein binding of rabbit IgG. In the
355 immunofluorescent figures, blue and red indicate nuclear staining by DAPI and
356 immunoreactivity to IL-18r1 and IL-1B, respectively. Scale bars indicate 100 μm (low-power
357 view) and 50 μm (insets showing the spiral ligament, spiral limbus, and organ of Corti).
358
359 Immunohistochemical analysis of the two NF-κB-interacting inflammatory molecules
360 (TNFα and PTGS2) showed that they were expressed ubiquitously in the cochlear structures
361 of the 12-month-old mice. Unequivocal immunoreactivity to TNFα and PTGS2 was observed
362 in the lateral wall (the spiral ligament and stria vascularis) of the aged cochleae (upper insets
363 in Fig 6). Cochlear localization of TNFα and PTGS2 in the 6-week-old mice was similar to that
364 in the 12-month-old mice (lower insets in Fig 6).
365
366 **Fig 6. Immunohistochemical analysis of tumor necrosis factor α (TNFα) and**
367 **prostaglandin-endoperoxide synthase 2 (PTGS2) expression in aged cochleae.** The
368 figures show immunoreactivity to TNFα and PTGS2 in the cochleae of 12-month-old and 6-
369 week-old mice. In the immunofluorescent figures, blue and red indicate nuclear staining by
370 DAPI and immunoreactivity to TNFα and PTGS2, respectively. Scale bars indicate 100 μm.
371
372 As shown in Fig 7, IBA1-positive macrophages were observed in the stria vascularis and

the inferior division of the spiral limbus in the cochleae of 12-month-old mice. No IBA1-positive cells were found in the cochlear structures of 6-week-old mice.

Fig 7. Immunohistochemistry showing IBA1-positive macrophages in aged cochleae. The figures show immunohistochemical detection of IBA1-positive macrophages in the stria vascularis and the inferior division of the spiral ligament in the cochleae of 12-month-old mice. No IBA1-positive cells were observed in the cochlear structures of 6-week-old mice. Blue and brown indicate nuclear staining by hematoxylin and immunoreactivity to IBA1, respectively. Negative control sections incubated with nonspecific rabbit IgG showed no signals. Scale bars indicate 50 μm.

Discussion

In this study, we hypothesized that inflammation and immune reactions are regulated during the aging process of mice cochlear tissues with ARHL. To test this hypothesis, we analyzed the expression levels of 84 key genes known to be involved in inflammatory and immune functions in aged and young cochleae. Of the 84 genes examined by a real-time RT-PCR array, the expressions of 40 (47.6%) were differentially regulated in the cochleae of 12-month-old compared with 6–7-week-old mice, 33 of which were upregulated in the aged cochleae. The results of our experiments supported the hypothesis that inflammatory and immune

392 reactions are modulated in aged cochlear tissues. The differential expressions of these
393 immune-related genes were involved in functional gene pathways such as cytokine–cytokine
394 receptor interaction, the chemokine signaling pathway, the TNF signaling pathway, and the
395 Toll-like receptor signaling pathway.

396 A transcription factor, NF-κB, was upregulated in the aged cochlear tissue and predicted
397 to bind to the genomic regulatory sequences of eight upregulated DEGs: *Ccl5*, *Cxcl10*, *Cxcl9*,
398 *Il1a*, *Lta*, *Ltb*, *Ptgs2*, and *Tnf*. In general, NF-κB is a master regulator controlling gene
399 expressions pertaining to innate immunity and plays a role in the aging process [20]. In
400 cochleae during the pathological processes of noise-induced hearing loss and ARHL, NF-κB
401 transcriptional activity was strongly induced in the spiral ligament and stria vascularis of the
402 lateral wall [21]. In the immunohistochemical analyses in the present study, two NF-κB-
403 interacting molecules, TNFα and PTGS2, were also expressed in the spiral ligament and stria
404 vascularis of the lateral wall in aged cochleae. Our gene expression analyses corroborated
405 the data that NF-κB may control the transcriptional network of immune-related genes during
406 the aging process of the cochlea.

407 In agreement with our data, recent study by Su et al. showed that the gene expressions
408 involved in inflammatory and immune functions were upregulated in the cochleae of 12-month-
409 old C57BL/6J mice as compared with 4-week-old mice by means of next-generation
410 sequencing (RNA-seq) [10]. However, they did not provide information on the age of mice

411 when the inflammatory and immunity-related gene expressions were modulated in the
412 cochleae during the aging process. Our data, obtained by gene-specific real-time RT-PCR,
413 provide new evidence that the major proinflammatory molecules *IL1B* and *IL18rap* are
414 significantly upregulated in cochleae at 3 and 6 months, respectively, and thereafter in aging
415 cochleae. Upregulation of an interferon-induced gene, *Ifit3*, was also observed at 3 months
416 and thereafter. Subsequently during the aging process, seven of the nine immune-related
417 genes examined in our experiments (*Casp1*, *IL18r1*, *IL1B*, *Card9*, *Clec4e*, *Ifit1*, and *Tlr9*)
418 showed significant upregulation between the late time points of 9 and 12 months. According
419 to a previously published paper [11], ABR thresholds in the high-frequency range (32 kHz) in
420 inbred C57BL/6J mice were 45.0 dB SPL at 3 months of age, and subsequently showed
421 threshold shifts of 33.1, 38.4, and 47.1 dB at 6, 9, and 12 months, respectively, compared with
422 the threshold at 3 months. Based on these observations, *IL1B*, *IL18rap*, and *Ifit3* may play
423 significant roles in the development of ARHL by 6 months of age. *IL1B* and the six other genes,
424 *Casp1*, *IL18r1*, *Card9*, *Clec4e*, *Ifit1*, and *Tlr9*, may participate in the immune response to the
425 degeneration of the cochlear cells because C57BL/6J mice exhibited significant ARHL as early
426 as 6 months of age [11]. These data suggest that a remarkable progression of the innate
427 immunity process occurred in mice cochleae at an advanced stage of ARHL (between 9 and
428 12 months of age).

429 By means of gene-specific RT-PCR, Shi et al. demonstrated upregulation of NOD-like

receptor family pyrin domain containing 3 (NLRP3) inflammasome genes (*Casp1*, *IL18*, and *IL1B*) in the cochleae of 12-month-old mice [9]. These NLRP3 inflammasome molecules, which were also examined in our gene-specific real-time RT-PCR, comprise a key innate immune pathway involved in the recognition of molecular triggers that appear during cellular senescence [22]. Among the genes analyzed in our experiments, *Card9* and *Clec4e* activated macrophage inflammatory responses, which may play roles in chronic inflammatory diseases [23, 24]. Both *Ifit1 and Ifit3* are interferon-inducible genes that control pro-inflammatory gene programming in macrophages [25, 26]. *Tlr9* recognizes its ligands of pathogenic DNA in immune cells and triggers signaling cascades that lead to the induction of type 1 interferon expression and pro-inflammatory cytokine responses [27].

The downregulation of seven immune-related genes—*Ccl1*, *Ccl20*, *Cxcl3*, *IL17a*, *IL22*, *IL9*, and *Crp*—was demonstrated by the RT-PCR array analysis in 12-month-old cochleae. The three downregulated chemokine-ligand genes—*Ccl1*, *Ccl20*, and *Cxcl3*—were closely related to each other in the gene expression network of the 40 DEGs shown in Fig 3. The three interleukins—*IL17*, *IL22*, and *IL9*—were also closely associated in the gene expression network. *Ccl1* and *IL9* are known to be involved in the anti-apoptotic activity of immune cells [28, 29].

In our immunohistochemical analyses, IL-18r1 and IL-1B proteins localized to the spiral ligament, spiral limbus, and organ of Corti in cochlear sections from aged mice. IL-18 and IL-

449 1B are major proinflammatory molecules that participate in the inflammasome pathway, and
450 RT-PCR analyses have shown that their encoding genes are upregulated in aged cochleae.
451 In a previous report, the expression of an inflammasome-forming protein, NLRP3 was
452 detected by immunohistochemistry in cochlear structures, including the spiral neurons, in aged
453 mice with ARHL [9]. These data therefore suggest that innate immune reactions play
454 significant roles in the aging process in these cochlear structures. In addition, IBA1-positive
455 macrophages were observed in the stria vascularis and the inferior division of the spiral
456 ligament. These lateral wall structures (the stria vascularis and the inferior division of the spiral
457 ligament) are thought to be the primary anatomical structure of leukocyte migration into the
458 cochleae because of their abundantly dense vasculature [30].

459 Chronic low-grade inflammation plays a key role in age-related diseases such as
460 Alzheimer's disease via a process called inflammaging [31]. An epidemiologic study of 611
461 older adults in the United Kingdom showed that increases in serum inflammatory markers,
462 including white blood cell count, neutrophil count, IL-6 levels, and C-reactive protein levels,
463 were significantly associated with worse hearing levels, as demonstrated statistically by
464 multiple regression models after adjusting for the covariates of age, gender, smoking status,
465 and exposure to noise at work [7]. Based on such data, a clinical trial was conducted to
466 investigate whether continuous oral administration of low-dose aspirin prevented or reduced
467 ARHL in a 3-year study [32]. In animal experiments aimed at developing immunologic ARHL

468 therapies, hearing loss, degeneration of the spiral neurons, and T-cell dysfunction observed
469 in 6-month-old mice recovered in 12-month-old mice that had received two fetal thymus
470 transplants [33].

471 A recent study by Srivastava et al. analyzed changes in the transcriptome using RNA-seq
472 in the brain, blood, skin, and liver of C57BL/6 mice at 9, 15, 24, and 30 months of age [34].
473 They found that the most significant DEGs in the aged brain, blood, and liver were upregulated
474 genes of inflammation and immune function. Compared with the brain, blood, and liver, only a
475 few genes of inflammation and immune function were differentially regulated in the aged skin.
476 We therefore speculate that DEGs involved in the immune system may be a common
477 characteristic found in the transcriptome of aged nervous systems, including the auditory
478 system. Age-related changes in the gene expressions unique to the cochlea might also be
479 present because of its direct exposure to environmental stress (noise).

480 The gene and protein expression data in this study showed that inflammatory and immune
481 reactions were modulated in aged cochlear tissues with ARHL. How these inflammatory and
482 immune reactions positively or negatively impact the pathologic mechanisms of ARHL should
483 be further clarified in animal experiments. These data could serve as the basis for the
484 development of preventive and therapeutic measures for treating ARHL by targeting immune
485 function in the cochleae.

486 A limitation of this study is that the expression levels of the NF-κB-interacting upregulated

genes (*Ccl5, Cxcl10, Cxcl9, Il1a, Lta, Ltb, Ptgs2, and Tnf*) were not analyzed by real-time RT-PCR at different ages (3-, 6-, 9-, and 12-month-old mice). Such data would provide important insights into the involvement of the NF-κB-interacting immune gene network in the molecular process of age-related hearing loss.

Acknowledgments: None.

References

1. National Institute on Deafness and Other Communication Disorders, Accessed in December, 2019. Age-Related Hearing Loss. https://www.nidcd.nih.gov/health/age-related-hearing-loss.

2. Cabinet office, Government of Japan, 2019. White book of aged society.

3. Livingston G, Huntley J, Sommerlad A, Ames D, Ballard C, Banerjee S, et al. Dementia prevention, intervention, and care: 2020 report of the Lancet Commission. Lancet. 2020;396(10248):413-46. PubMed PMID: 32738937.

4. Rizk HG, Linthicum FH, Jr. Histopathologic categorization of presbycusis. Otol Neurotol. 2012;33(3):e23-4. PubMed PMID: 21659923.

5. Someya S, Yamasoba T, Prolla TA, Tanokura M. Genes encoding mitochondrial respiratory chain components are profoundly down-regulated with aging in the cochlea of DBA/2J mice. Brain Res. 2007;1182:26-33. PubMed PMID: 17964557.

6. Yamasoba T, Lin FR, Someya S, Kashio A, Sakamoto T, Kondo K. Current concepts in age-related hearing loss: epidemiology and mechanistic pathways. Hear Res. 2013;303:30-8. PubMed PMID: 23422312.

7. Verschuur CA, Dowell A, Syddall HE, Ntani G, Simmonds SJ, Baylis D, et al. Markers of inflammatory status are associated with hearing threshold in older people: findings from the Hertfordshire Ageing Study. Age Ageing. 2012;41(1):92-7. PubMed PMID: 22086966.

8. Nash SD, Cruickshanks KJ, Zhan W, Tsai MY, Klein R, Chappell R, et al. Long-term assessment of systemic inflammation and the cumulative incidence of age-related hearing impairment in the epidemiology of hearing loss study. J Gerontol A Biol Sci Med Sci. 2014;69(2):207-14. PubMed PMID: 23739996.

9. Shi X, Qiu S, Zhuang W, Yuan N, Wang C, Zhang S, et al. NLRP3-inflammasomes are triggered by age-related hearing loss in the inner ear of mice. Am J Transl Res. 2017;9(12):5611-8. PubMed PMID: 29312513.

10. Su Z, Xiong H, Liu Y, Pang J, Lin H, Zhang W, et al. Transcriptomic analysis highlights cochlear inflammation associated with age-related hearing loss in C57BL/6 mice using next generation sequencing. PeerJ. 2020;8:e9737. PubMed PMID: 32879802.

11. Kane KL, Longo-Guess CM, Gagnon LH, Ding D, Salvi RJ, Johnson KR. Genetic background effects on age-related hearing loss associated with Cdh23 variants in mice. Hear Res. 2012;283(1-2):80-8. PubMed PMID: 22138310.

12. Maeda Y, Fukushima K, Omichi R, Kariya S, Nishizaki K. Time courses of changes in phospho- and total- MAP kinases in the cochlea after intense noise exposure. PLoS One. 2013;8(3):e58775. PubMed PMID: 23484051.

13. Huang DW, Sherman BT, Lempicki RA. Systematic and integrative analysis of large gene lists using DAVID Bioinformatics Resources. Nature Protoc. 2009;4:44-57. PubMed PMID: 19131956.

14. Huang DW, Sherman BT, Lempicki RA. Bioinformatics enrichment tools: paths toward the comprehensive functional analysis of large gene lists. Nucleic Acids Res. 2009;37:1-13. PubMed PMID: 19033363.

15. Mootha VK, Lindgren CM, Eriksson KF, Subramanian A, Sihag S, Lehar J, et al. PGC-1alpha-responsive genes involved in oxidative phosphorylation are coordinately downregulated in human diabetes. Nat Genet. 2003;34(3):267-73. PubMed PMID: 12808457.

16. Subramanian A, Tamayo P, Mootha VK, Mukherjee S, Ebert BL, Gillette MA, et al. Gene set enrichment analysis: a knowledge-based approach for interpreting genome-wide expression profiles. Proc Natl Acad Sci U S A. 2005;102(43):15545-50. PubMed PMID: 16199517.

17. Szklarczyk D, Gable AL, Lyon D, Junge A, Wyder S, Huerta-Cepas J, et al. STRING v11: protein-protein association networks with increased coverage, supporting functional discovery in genome-wide experimental datasets. Nucleic Acids Res. 2019;47(D1):D607-D13. PubMed PMID: 30476243.

18. Kanazawa H, Ohsawa K, Sasaki Y, Kohsaka S, Imai Y. Macrophage/microglia-specific protein Iba1 enhances membrane ruffling and Rac activation via phospholipase C-gamma -dependent pathway. J Biol Chem. 2002;277(22):20026-32. PubMed PMID: 11916959.

19. Spongr VP, Flood DG, R.D. F, Salvi RJ. Quantitative Measures of Hair Cell Loss in CBA and C57BL/6 Mice Throughout Their Life Spans. J Acoust Soc Am. 1997;101(6):3546-53. PubMed PMID: 9193043.

20. Salminen A, Huuskonen J, Ojala J, Kauppinen A, Kaarniranta K, Suuronen T. Activation of innate immunity system during aging: NF-kB signaling is the molecular culprit of inflamm-aging. Ageing Res Rev. 2008;7(2):83-105. PubMed PMID: 17964225.

21. Herranen A, Ikaheimo K, Virkkala J, Pirvola U. The Stress Response in the Non-sensory Cells of the Cochlea Under Pathological Conditions-Possible Role in Mediating Noise Vulnerability. J Assoc Res Otolaryngol. 2018;19(6):637-52. PubMed PMID: 30191426.

22. Latz E, Duewell P. NLRP3 inflammasome activation in inflammaging. Semin Immunol. 2018;40:61-73. PubMed PMID: 30268598.

23. Drouin M, Saenz J, Chiffoleau E. C-Type Lectin-Like Receptors: Head or Tail in Cell Death Immunity. Front Immunol. 2020;11:251. PubMed PMID: 32133013.

24. Ruland J. CARD9 signaling in the innate immune response. Ann N Y Acad Sci. 2008;1143:35-44. PubMed PMID: 19076343.

25. John SP, Sun J, Carlson RJ, Cao B, Bradfield CJ, Song J, et al. IFIT1 Exerts

Opposing Regulatory Effects on the Inflammatory and Interferon Gene Programs in LPS-Activated Human Macrophages. Cell Rep. 2018;25(1):95-106 e6. PubMed PMID: 30282041.

26. Huang C, Lewis C, Borg NA, Canals M, Diep H, Drummond GR, et al. Proteomic Identification of Interferon-Induced Proteins with Tetratricopeptide Repeats as Markers of M1 Macrophage Polarization. J Proteome Res. 2018;17(4):1485-99. PubMed PMID: 29508616.

27. Holm CK, Paludan SR, Fitzgerald KA. DNA recognition in immunity and disease. Curr Opin Immunol. 2013;25(1):13-8. PubMed PMID: 23313533.

28. Louahed J, Struyf S, Demoulin JB, Parmentier M, Van Snick J, Van Damme J, et al. CCR8-dependent activation of the RAS/MAPK pathway mediates anti-apoptotic activity of I-309/ CCL1 and vMIP-I. Eur J Immunol. 2003;33(2):494-501. PubMed PMID: 12645948.

29. Parrot T, Allard M, Oger R, Benlalam H, Raingeard de la Bletiere D, Coutolleau A, et al. IL-9 promotes the survival and function of human melanoma-infiltrating CD4(+) CD8(+) double-positive T cells. Eur J Immunol. 2016;46(7):1770-82. PubMed PMID: 27094152.

30. Sahley TL, Anderson DJ, Hammonds MD, Chandu K, Musiek FE. Evidence for a dynorphin-mediated inner ear immune/inflammatory response and glutamate-induced neural excitotoxicity: an updated analysis. J Neurophysiol. 2019;122(4):1421-60. PubMed PMID: 31339807.

31. Salminen A. Activation of immunosuppressive network in the aging process. Ageing Res Rev. 2020;57:100998. Epub 2019/12/16. doi: 10.1016/j.arr.2019.100998. PubMed PMID: 31838128.

32. Lowthian JA, Britt CJ, Rance G, Lin FR, Woods RL, Wolfe R, et al. Slowing the progression of age-related hearing loss: Rationale and study design of the ASPIRIN in HEARING, retinal vessels imaging and neurocognition in older generations (ASPREE-HEARING) trial. Contemp Clin Trials. 2016;46:60-6. PubMed PMID: 26611434.

33. Iwai H, Inaba M. Fetal thymus graft enables recovery from age-related hearing loss and expansion of CD4-Positive T cells expressing IL-1 receptor type 2 and regulatory T Cells. Immun Ageing. 2015;12:26. PubMed PMID: 26673738.

34. Srivastava A, Barth E, Ermolaeva MA, Guenther M, Frahm C, Marz M, et al. Tissue-specific Gene Expression Changes Are Associated with Aging in Mice. Genomics

Proteomics Bioinformatics. 2020. PubMed PMID: 33309863.

Supporting information captions

S1 Table. Gene symbols, names, and cochlear expressions of the 84 immune-related genes examined by real-time RT-PCR array in this study. The expressions of inflammatory and immune-related genes in the cochleae of 12-month-old relative to 6–7-week-old mice are tabulated. The expressions of 84 immune-related genes were analyzed by real-time RT-PCR array. As a result, 33 upregulated and 7 downregulated genes were detected with greater than a twofold or less than a 0.5-fold change, respectively, with a *P*-value <0.05 for significantly different expression levels between the 12-month-old and 6–7-week-old mice (*n*=3, *t*-test).

Expressions of inflammatory and immune-related genes in cochleae of 12-month-old mice compared to 6- to 7-week-old mice									
				Regulation					Regulation
Gene symbol	Gene name	P-value (*t*-test)	Fold change	in aged cochleae	Gene symbol	Gene name	P-value (*t*-test)	Fold change	in aged cochleae
Bcl6	B-cell leukemia/lymphoma 6	0.01496	1.42		*Ifng*	Interferon gamma	0.01286	2.22	up
C3	Complement component 3	0.01015	1.55		*Il10*	Interleukin 10	0.01620	0.66	
C3ar1	Complement component 3a receptor 1	0.00008	1.57		*Il10rb*	Interleukin 10 receptor, beta	0.04427	1.3	
C4b	Complement component 4B (Childo blood group)	0.00901	1.77		*Il17a*	Interleukin 17A	0.00017	0.38	down
Ccl1	Chemokine (C-C motif) ligand 1	0.00014	0.39	down	*Il18*	Interleukin 18	0.02579	1.48	
Ccl11	Chemokine (C-C motif) ligand 11	0.75093	0.96		*Il1a*	Interleukin 1 alpha	0.00470	2.32	up
Ccl12	Chemokine (C-C motif) ligand 12	0.00034	3.48	up	*Il1b*	Interleukin 1 beta	0.00053	3.67	up
Ccl17	Chemokine (C-C motif) ligand 17	0.02244	1.76		*Il1r1*	Interleukin 1 receptor, type I	0.36098	1.07	
Ccl19	Chemokine (C-C motif) ligand 19	0.00289	0.74		*Il1rap*	Interleukin 1 receptor accessory protein	0.36061	0.81	
Ccl2	Chemokine (C-C motif) ligand 2	0.00065	3.31	up	*Il1rn*	Interleukin 1 receptor antagonist	0.05258	1.62	
Ccl20	Chemokine (C-C motif) ligand 20	0.00014	0.39	down	*Il22*	Interleukin 22	0.00014	0.39	down
Ccl22	Chemokine (C-C motif) ligand 22	0.04276	1.3		*Il23a*	Interleukin 23, alpha subunit p19	0.26433	0.76	
Ccl24	Chemokine (C-C motif) ligand 24	0.00899	1.29		*Il23r*	Interleukin 23 receptor	0.01648	1.59	
Ccl25	Chemokine (C-C motif) ligand 25	0.06898	0.88		*Il5*	Interleukin 5	0.02238	0.68	
Ccl3	Chemokine (C-C motif) ligand 3	0.37442	1.14		*Il6*	Interleukin 6	0.00002	4.43	up
Ccl4	Chemokine (C-C motif) ligand 4	0.03654	1.35		*Il6ra*	Interleukin 6 receptor, alpha	0.05990	1.42	
Ccl5	Chemokine (C-C motif) ligand 5	0.00124	3.2	up	*Il7*	Interleukin 7	0.00342	2.59	up
Ccl7	Chemokine (C-C motif) ligand 7	0.00037	2.38	up	*Il9*	Interleukin 9	0.00011	0.42	down
Ccl8	Chemokine (C-C motif) ligand 8	0.00173	11.24	up	*Itgb2*	Integrin beta 2	0.04342	1.69	
Ccr1	Chemokine (C-C motif) receptor 1	0.00130	2.72	up	*Kng1*	Kininogen 1	0.00136	4.26	up
Ccr2	Chemokine (C-C motif) receptor 2	0.00005	3.2	up	*Lta*	Lymphotoxin A	0.00301	2.83	up
Ccr3	Chemokine (C-C motif) receptor 3	0.00040	2.83	up	*Ltb*	Lymphotoxin B	0.00140	2.2	up
Ccr4	Chemokine (C-C motif) receptor 4	0.37273	1.14		*Ly96*	Lymphocyte antigen 96	0.03864	1.23	
Ccr7	Chemokine (C-C motif) receptor 7	0.00010	3.31	up	*Myd88*	Myeloid differentiation primary response gene 88	0.00013	1.63	
Cd14	CD14 antigen	0.00052	1.73		*Nfkb1*	Nuclear factor of kappa light polypeptide gene enhancer in B-cells 1, p10	0.00005	2.03	up
Cd40	CD40 antigen	0.01673	1.91		*Nos2*	Nitric oxide synthase 2, inducible	0.04560	0.65	
Cd40lg	CD40 ligand	0.01803	0.70		*Nr3c1*	Nuclear receptor subfamily 3, group C, member 1	0.00346	2.08	up
Cebpb	CCAAT/enhancer binding protein (C/EBP), beta	0.95456	1.01		*Ptgs2*	Prostaglandin-endoperoxide synthase 2	0.00477	2.59	up
Crp	C-reactive protein, pentraxin-related	0.00005	0.43	down	*Ripk2*	Receptor (TNFRSF)-interacting serine-threonine kinase 2	0.00241	1.94	
Csf1	Colony stimulating factor 1 (macrophage)	0.02641	1.4		*Sele*	Selectin, endothelial cell	0.03442	2.05	up
Cxcl1	Chemokine (C-X-C motif) ligand 1	0.04688	1.2		*Tirap*	Toll-interleukin 1 receptor (TIR) domain-containing adaptor protein	0.13878	1.24	
Cxcl10	Chemokine (C-X-C motif) ligand 10	0.00012	3.85	up	*Tlr1*	Toll-like receptor 1	0.00074	4.34	up
Cxcl11	Chemokine (C-X-C motif) ligand 11	0.71118	1.03		*Tlr2*	Toll-like receptor 2	0.06232	1.38	
Cxcl2	Chemokine (C-X-C motif) ligand 2	0.25655	0.81		*Tlr3*	Toll-like receptor 3	0.00016	1.71	
Cxcl3	Chemokine (C-X-C motif) ligand 3	0.00352	0.26	down	*Tlr4*	Toll-like receptor 4	0.00120	1.88	
Cxcl5	Chemokine (C-X-C motif) ligand 5	0.00264	1.56		*Tlr5*	Toll-like receptor 5	0.00014	1.36	
Cxcl9	Chemokine (C-X-C motif) ligand 9	0.00009	5.9	up	*Tlr6*	Toll-like receptor 6	0.00108	5.99	up
Cxcr1	Chemokine (C-X-C motif) receptor 1	0.00037	4.83	up	*Tlr7*	Toll-like receptor 7	0.00000	5.04	up
Cxcr2	Chemokine (C-X-C motif) receptor 2	0.00059	3.15	up	*Tlr9*	Toll-like receptor 9	0.00011	3.82	up
Cxcr4	Chemokine (C-X-C motif) receptor 4	0.00024	3.47	up	*Tnf*	Tumor necrosis factor	0.00149	2.06	up
Fasl	Fas ligand (TNF superfamily, member 6)	0.02733	2.67	up	*Tnfsf14*	Tumor necrosis factor (ligand) superfamily, member 14	0.00167	2.48	up
Fos	FBJ osteosarcoma oncogene	0.92637	1		*Tollip*	Toll interacting protein	0.54298	0.64	

Fig 1.

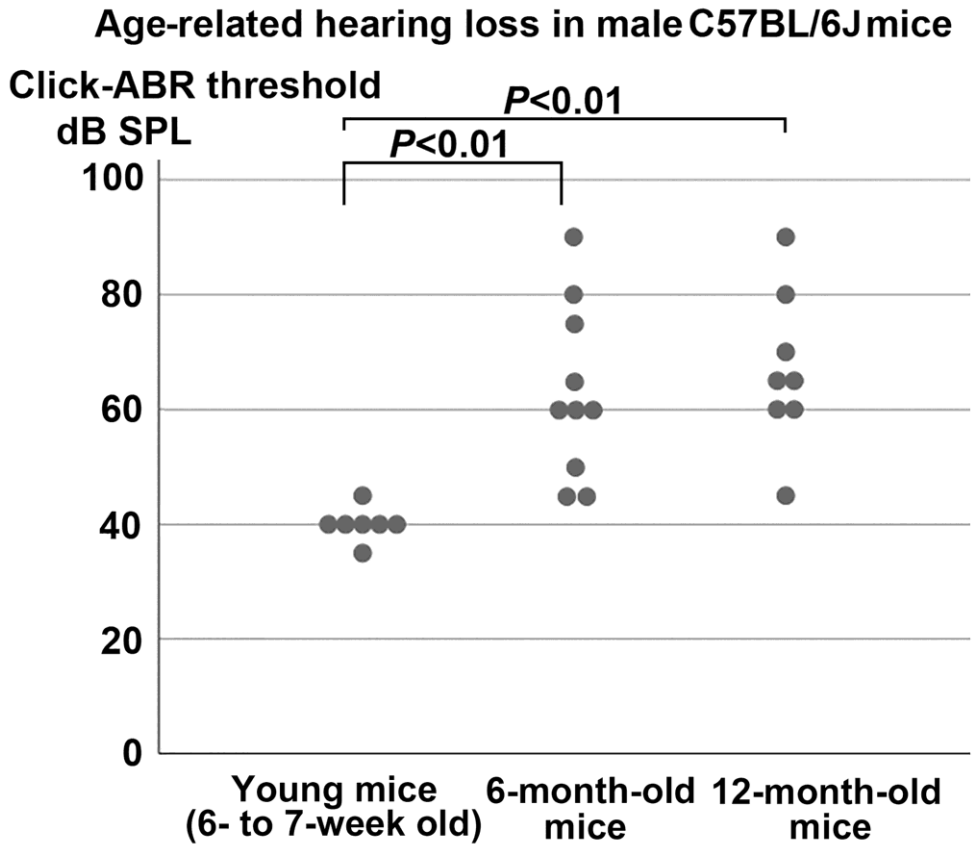

643

644 Fig. 2

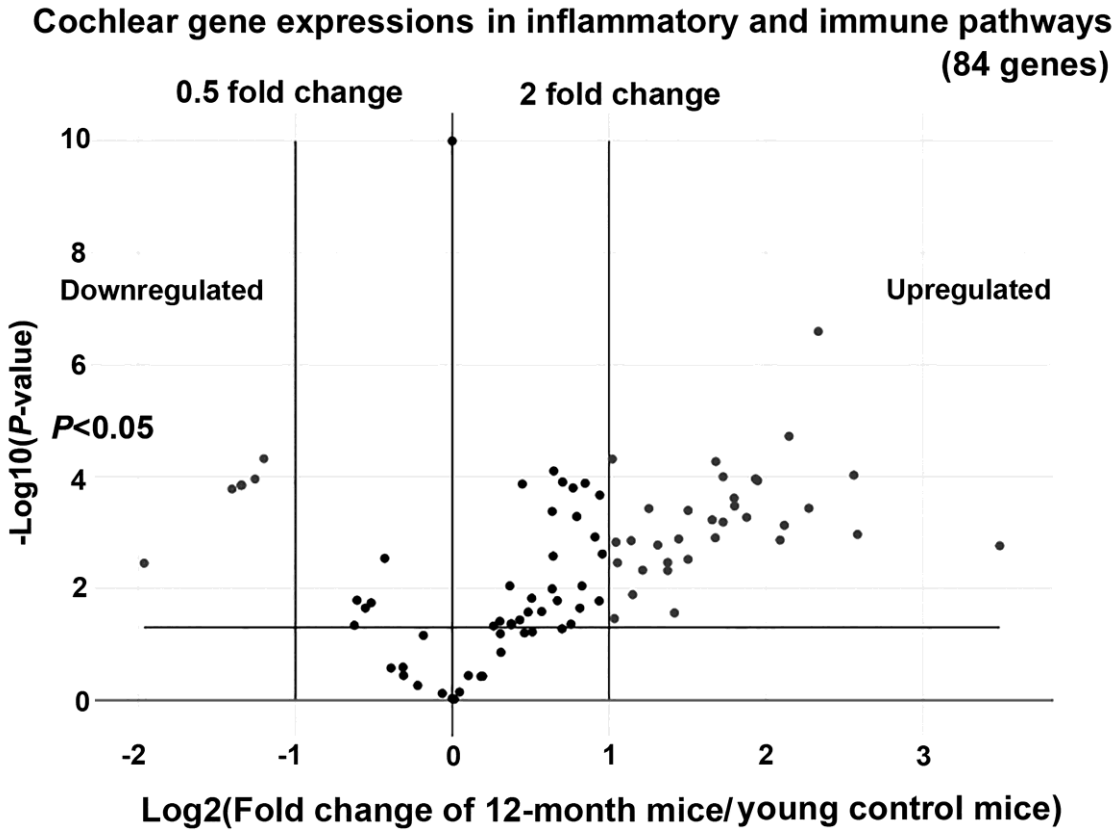

645

646

Fig. 3

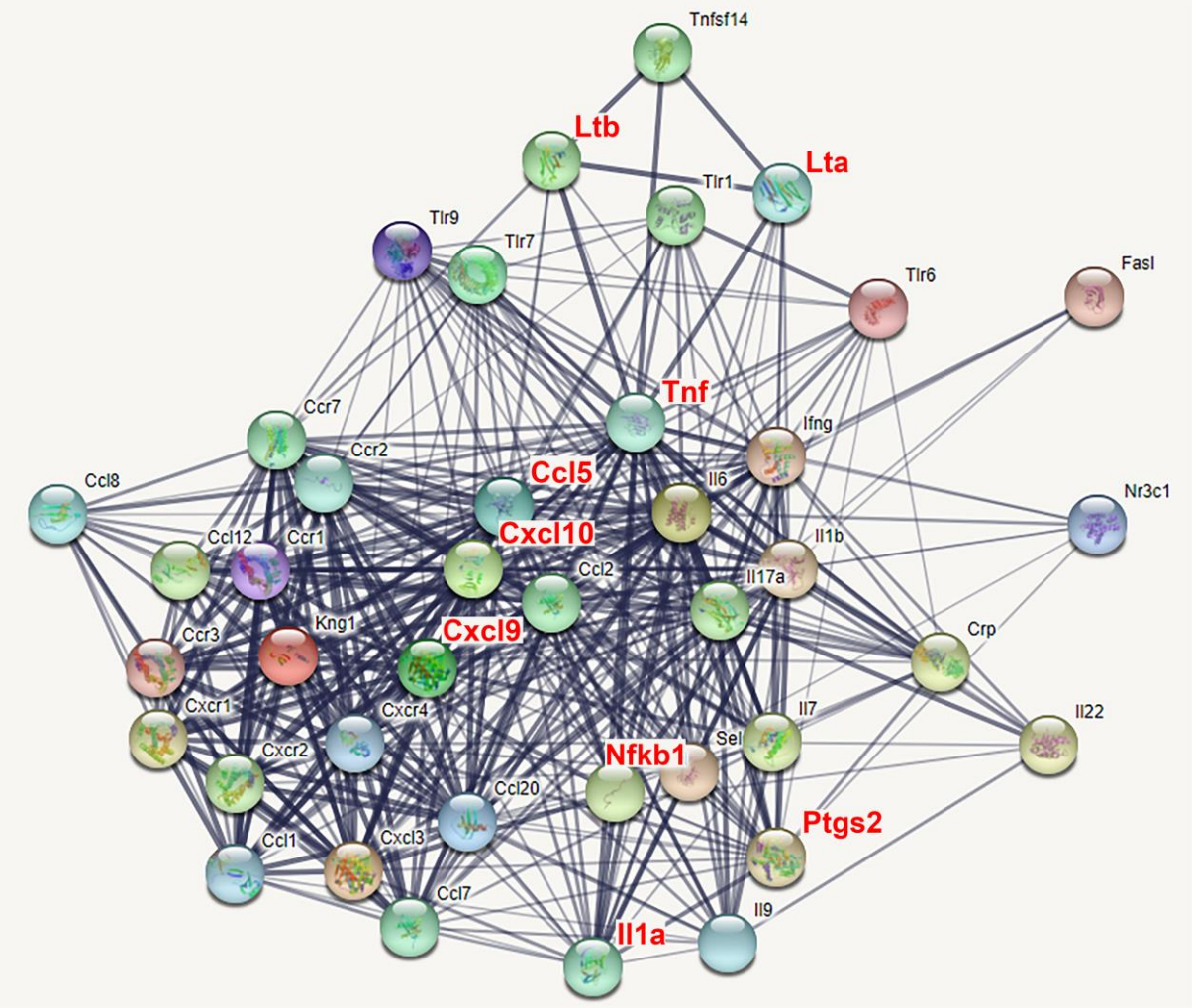
Tnfsf14
Ltb
Lta
Tlr1
Tlr9
Tlr7
Tlr6
Fasl
Tnf
Ccr7
Ifng
Ccr2
Ccl8
Ccl5
Il6
Nr3c1
Ccl12
Ccr1
Cxcl10
Il1b
Ccl2
Il17a
Ccr3
Kng1
Cxcl9
Crp
Cxcr1
Cxcr4
Il7
Il22
Sel
Cxcr2
Nfkb1
Ccl20
Ptgs2
Ccl1
Cxcl3
Ccl7
Il9
Il1a

664 Fig 4.

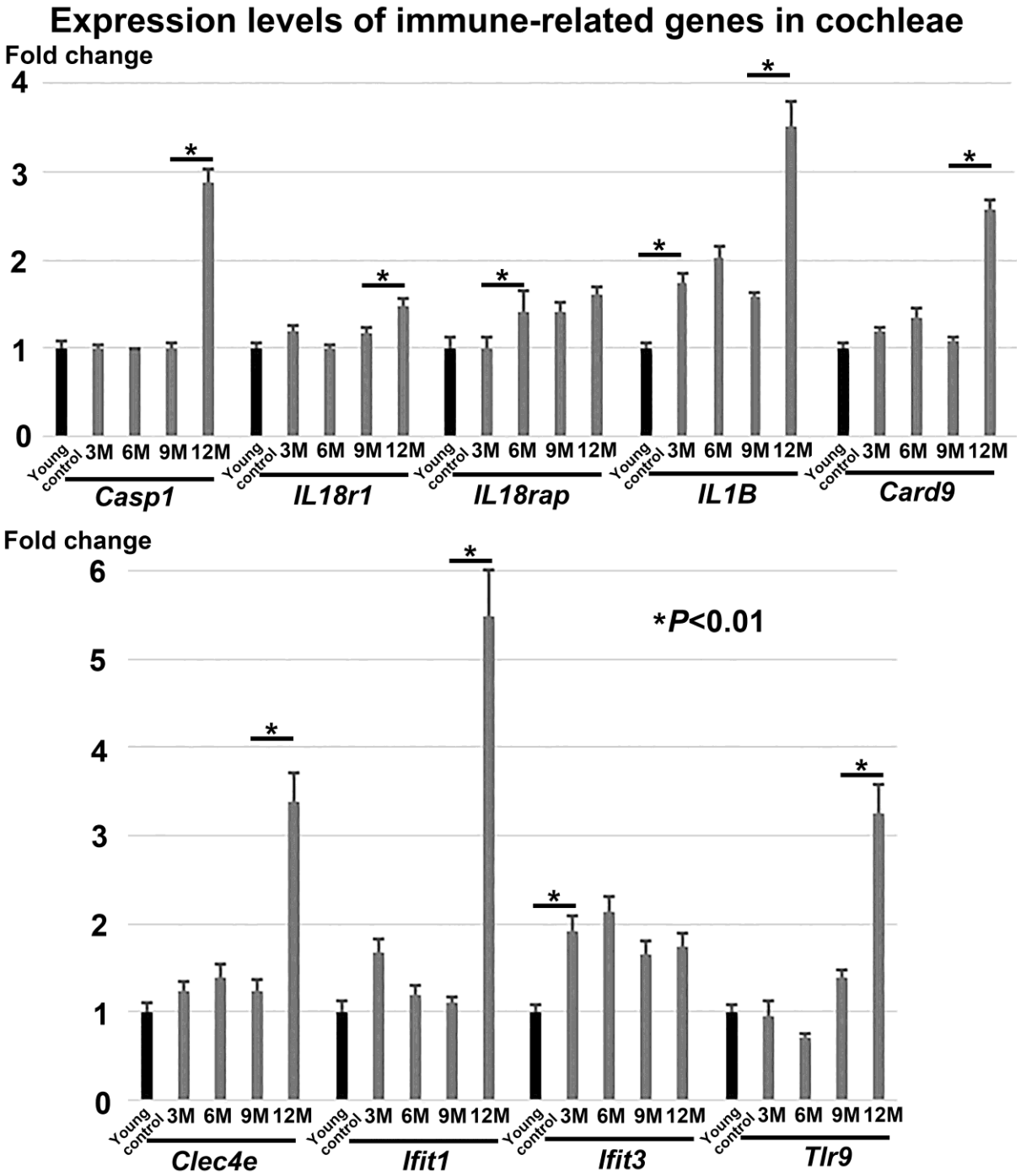

665
666
667
668
669
670
671
672

673 Fig 5.

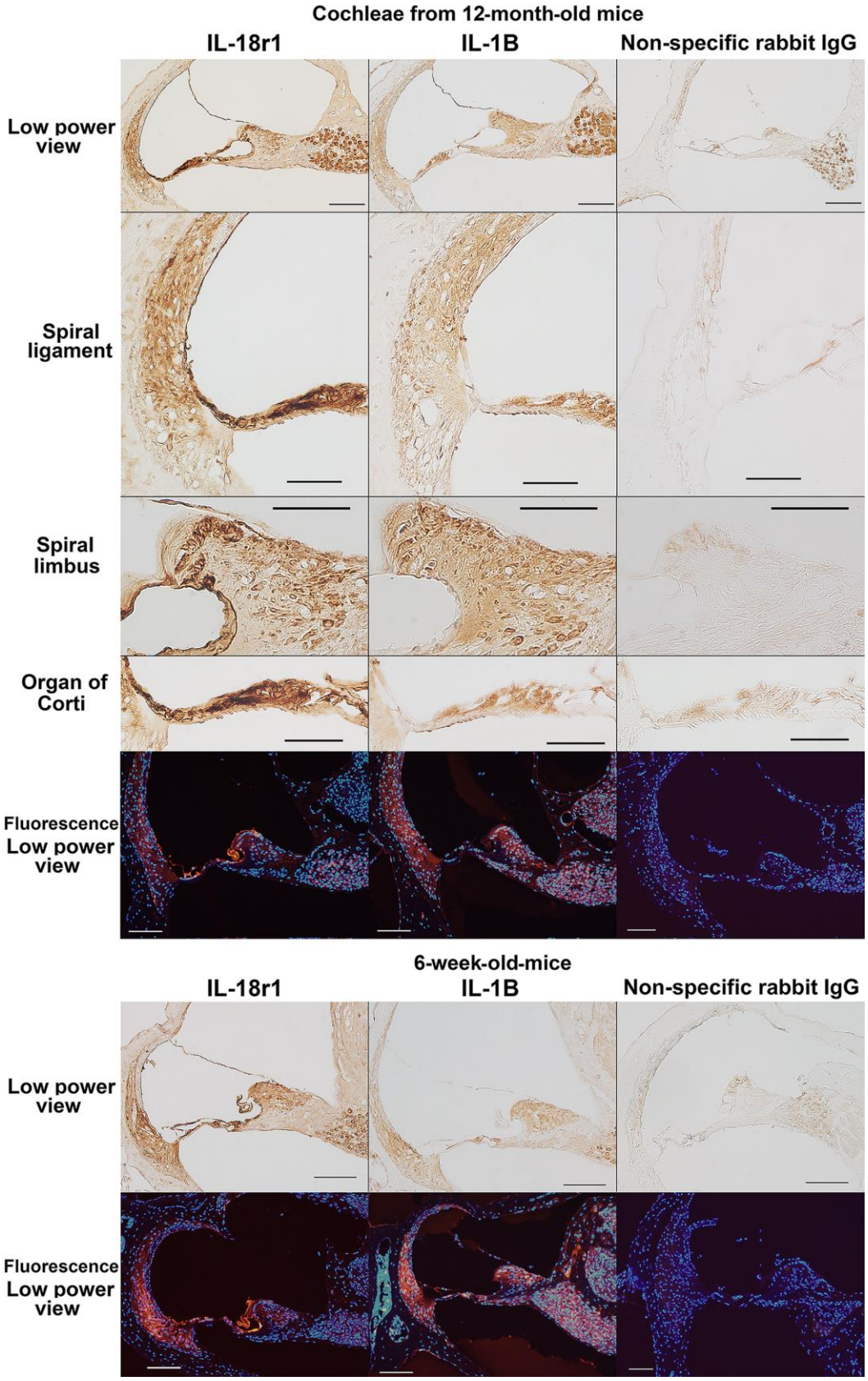

674
675
676

677 Fig 6.

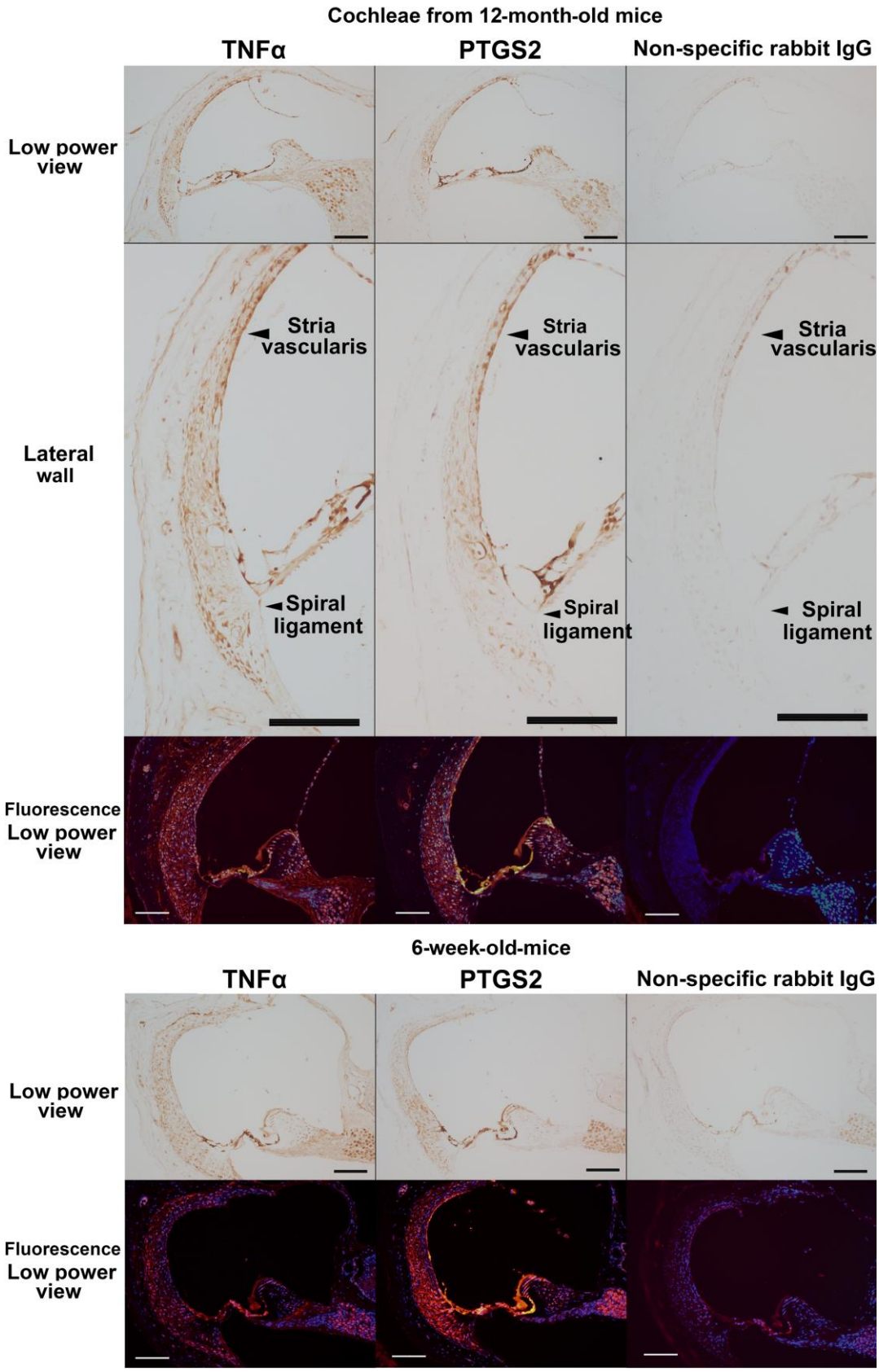

678
679
680

681 Fig 7.

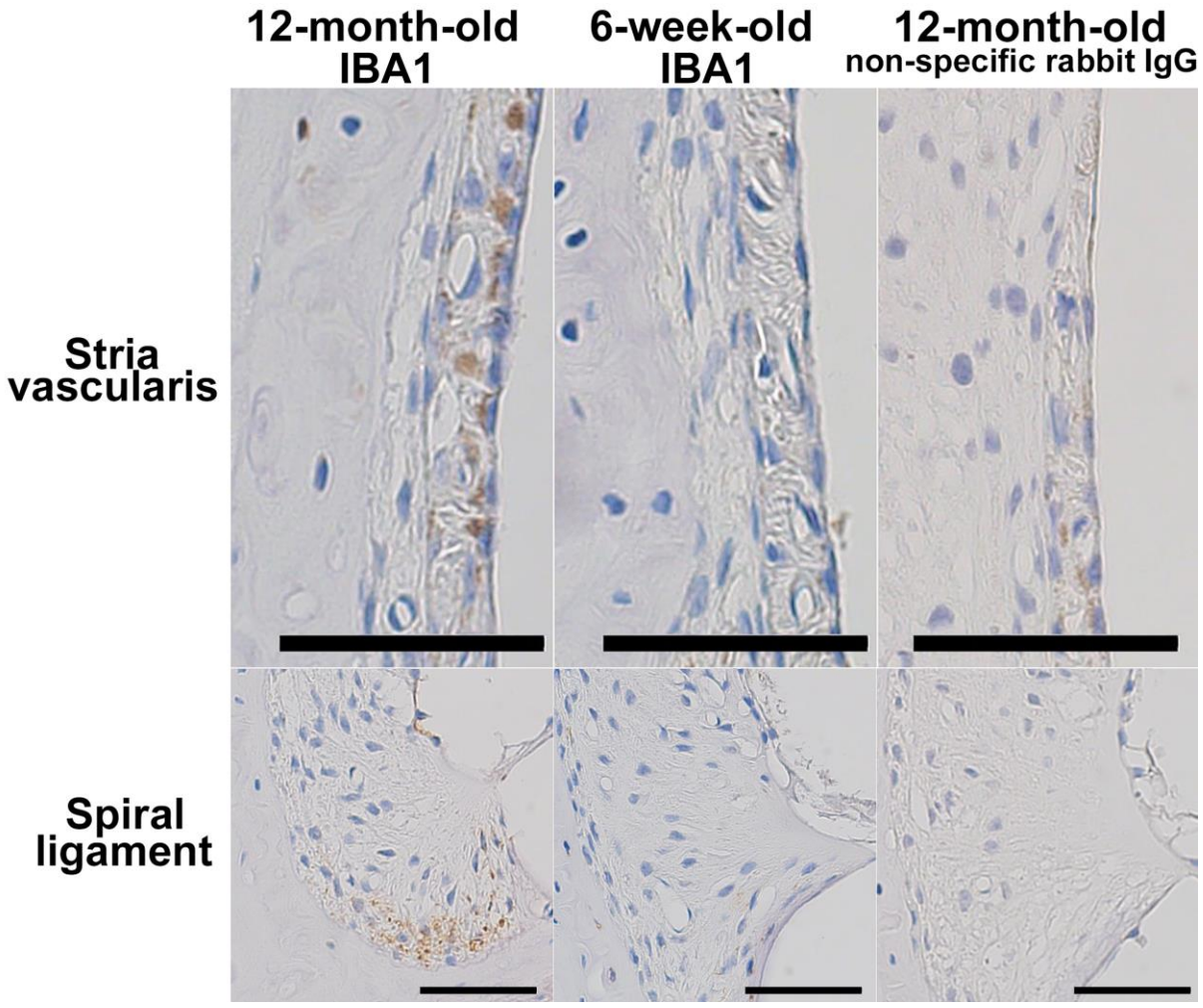
12-month-old
IBA1
6-week-old
IBA1
12-month-old
non-specific rabbit IgG
Stria
vascularis
Spiral
ligament

682